Supplementary Material (ESI) for Journal of Materials Chemistry

Electronic Supplementary Information

For the manuscript

Nanoporous Copolymer Networks Through Multiple Friedel-Crafts-Alkylation - Studies on Methane and Hydrogen Storage

by

Matthias Georg Schwab,*[a] Angela Lennert,[b,d]

Jörg Pahnke,[b] Gerhard Jonschker,[b] Matthias Koch,[b] Irena Senkovska,[c] Matthias Rehahn[d] and Stefan Kaskel*[c]

[a]Max Planck Institute for Polymer Research
Ackermannweg 10, D-55128 Mainz, Germany
schwab@mpip-mainz.mpg.de

[b]Merck KGaA
Frankfurter Straße 250, D-64293 Darmstadt, Germany

[c]Dresden University of Technology
Department of Inorganic Chemistry
Bergstraße 66, D-01062 Dresden, Germany
stefan.kaskel@chemie.tu-dresden.de

[d]Darmstadt University of Technology
Ernst-Berl-Institute for Technical and Macromolecular Chemistry
Petersenstraße 22, D-64287 Darmstadt, Germany

Materials and methods

The starting materials were purchased from Aldrich (4,4'-bis(chloromethyl)biphenyl, iron(III)chloride), ABCR (fluorene), Merck (9,9'-spirobi(fluorene), dibenzofuran, dibenzothiophene, 1,2-dichloroethane). The compounds were used as received without further purification.

Fourier transform infrared (FTIR) spectra were collected using KBr pellets on a Bruker Equinox55 spectrometer.

SEM measurements were performed on a Carl Zeiss Supra 35 scanning electron microscope.

^{13}C [1H] cross-polarization magic angle spinning (CP-MAS) NMR spectra were measured on a Bruker Avance 400 operating at 100.68 MHz for ^{13}C and 400.4 for ^{1}H. The NMR experiments were carried out at MAS of 10.0 kHz using zirconia rotors of 4 mm in diameter.

Nitrogen adsorption experiments and micropore analysis were conducted at 77 K using an ASAP 2420 from Micromeritics and a Quantachrome Autosorb1C apparatus. Before adsorption measurements, the samples were degassed in vacuum at 473 K for 12 h. Pore volumes at $p/p_0 = 0.1$ and $p/p_0 = 0.8$ were converted into the corresponding liquid volumes using a nitrogen density of $1.25 \cdot 10^{-3}$ g/cm^3 (gaseous) and $8.10 \cdot 10^{-1}$ g/cm^3 (liquid).

Low pressure hydrogen adsorption isotherms were measured at 77 K up to 1 bar using a Quantachrome Autosorb1C apparatus. Before adsorption measurements, the samples were degassed in vacuum at 473 K for 12 h. Gravimetric storage capacities were calculated using a hydrogen density of $8.99 \cdot 10^{-5}$ g/cm^3 (gaseous).

High-pressure methane adsorption measurements were conducted at room temperature using a Rubotherm magnetic suspension balance. Prior to the measurements, the samples were degassed at 473 K for 12 h.

High purity gases were used for the adsorption measurements (nitrogen: 99.999 %, hydrogen: 99.999 %, methane: 99.5 %).

Experimental section

General synthetic procedure

4,4'-bis(chloromethyl)biphenyl and the corresponding comonomer (see tables below) are dissolved in 40 ml of dry 1,2-dichloroethane. The solution is degassed by argon bubbling and iron(III)chloride is added. Subsequently, the reaction mixture is heated to 80 °C for 18 h under an inert atmosphere. The resulting precipitate is collected by filtration and thoroughly washed with water, methanol and methyl *tert*-butyl ether. The samples are dried at 80 °C under reduced pressure.

Table S1. Networks containing 10 mol% of comonomer.

	FLUO-10	**sFLUO-10**	**DBF-10**	**DBT-10**
BCMBP [mmol]	3.71	3.49	3.71	3.68
BCMBP [mg]	981	923	980	973
comonomer [mmol]	0.41	0.39	0.41	0.41
comonomer [mg]	70	124	71	77
iron(III)chloride [mmol]	4.12	3.88	4.12	4.09
iron(III)chloride [mg]	682	642	682	678

Table S2. Networks containing 25 mol% of comonomer.

	FLUO-25	**sFLUO-25**	**DBF-25**	**DBT-25**
BCMBP [mmol]	3.26	2.80	3.26	3.20
BCMBP [mg]	862	741	861	846
comonomer [mmol]	1.09	0.93	1.09	1.07
comonomer [mg]	184	299	188	201
iron(III)chloride [mmol]	4.35	3.73	4.35	4.27
iron(III)chloride [mg]	719	618	718	706

Fourier-Transform Infrared Spectroscopy (FTIR)

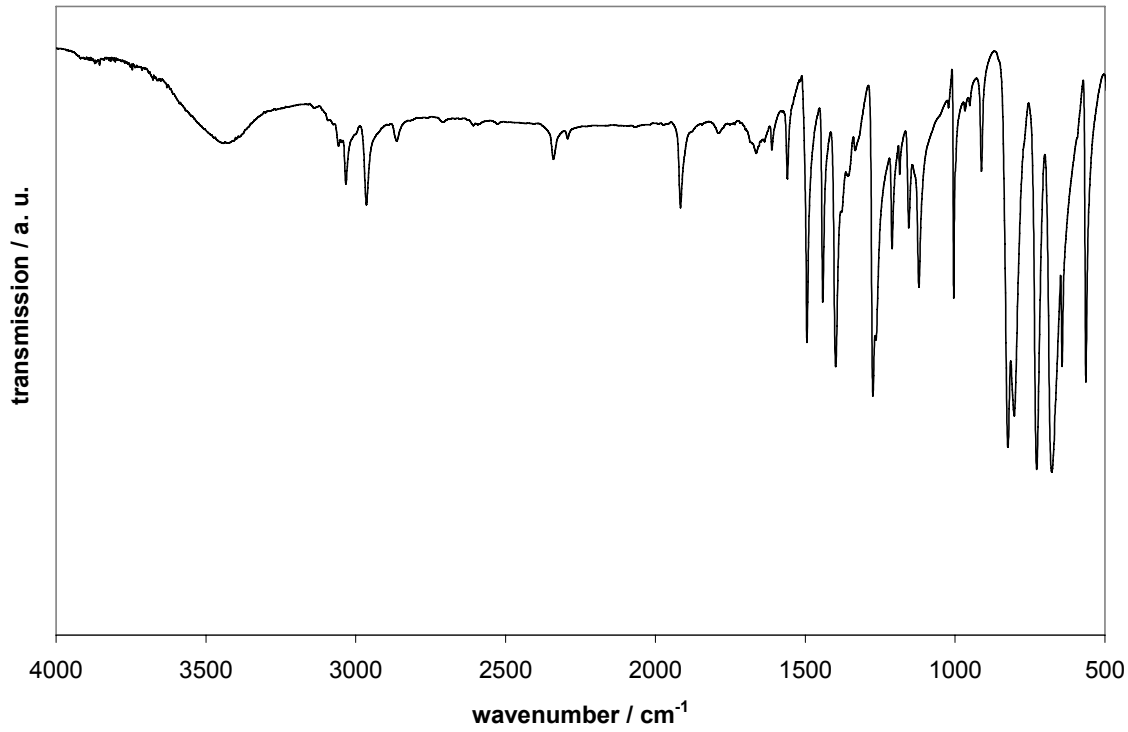

Figure S1. Fourier transform infrared (FTIR) spectra of the monomer **BCMBP**.

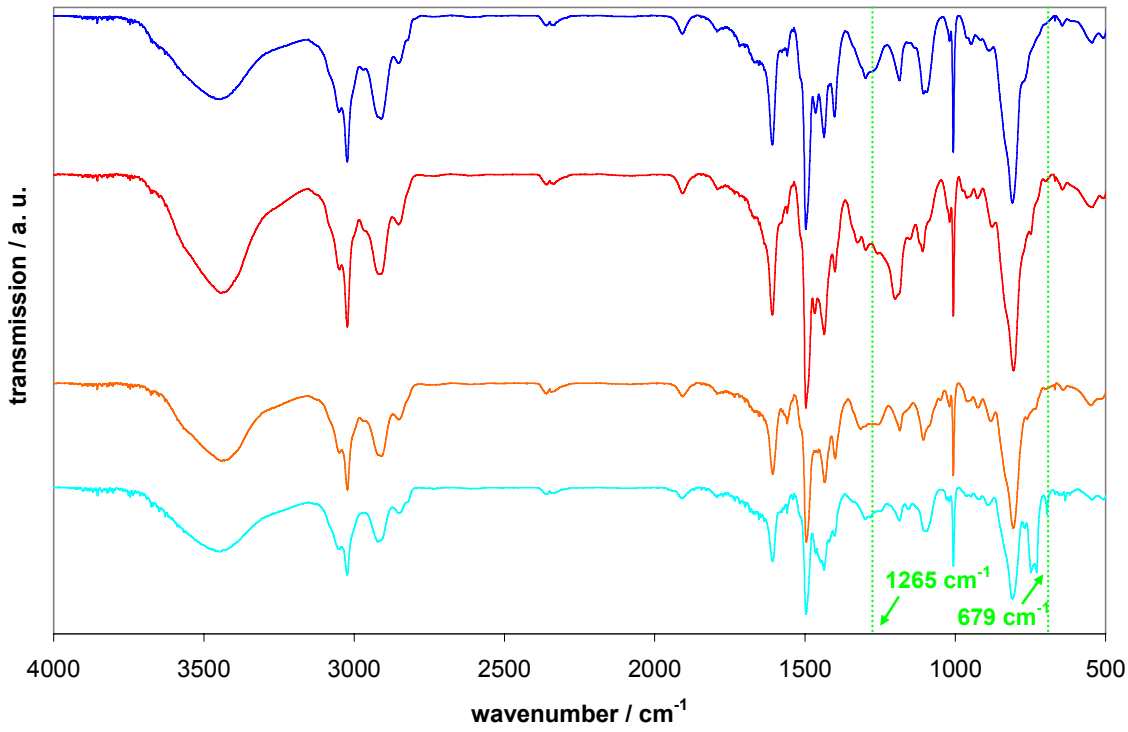

Figure S2. Fourier transform infrared (FTIR) spectra of **FLUO-25**, **sFLUO-25**, **DBF-25** and **DBT-25**.

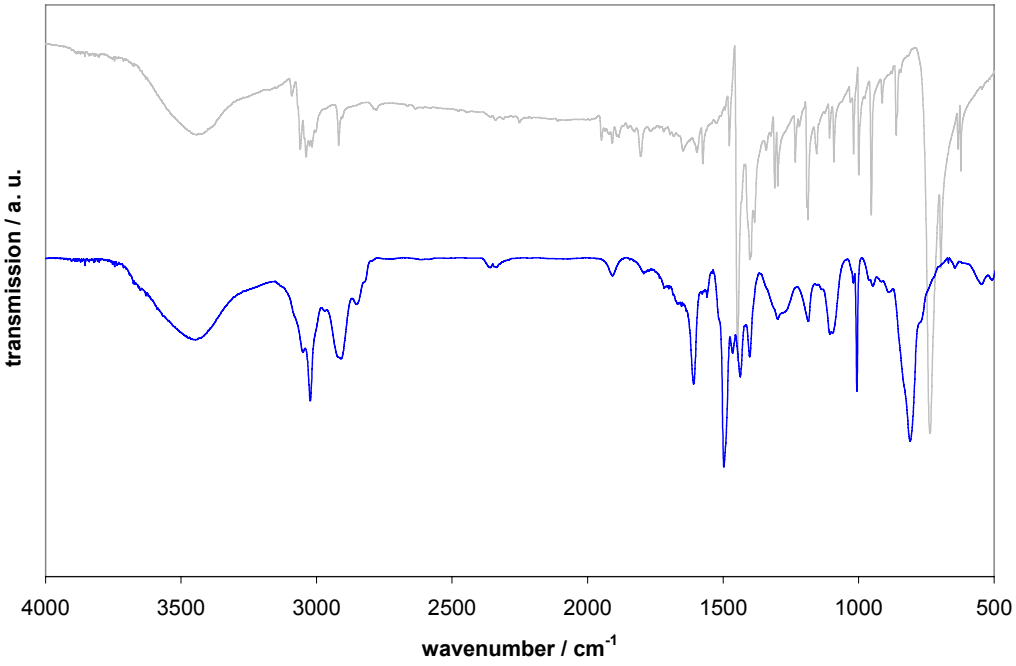

Figure S3. Fourier transform infrared (FTIR) spectra of **FLUO** and **FLUO-25**.

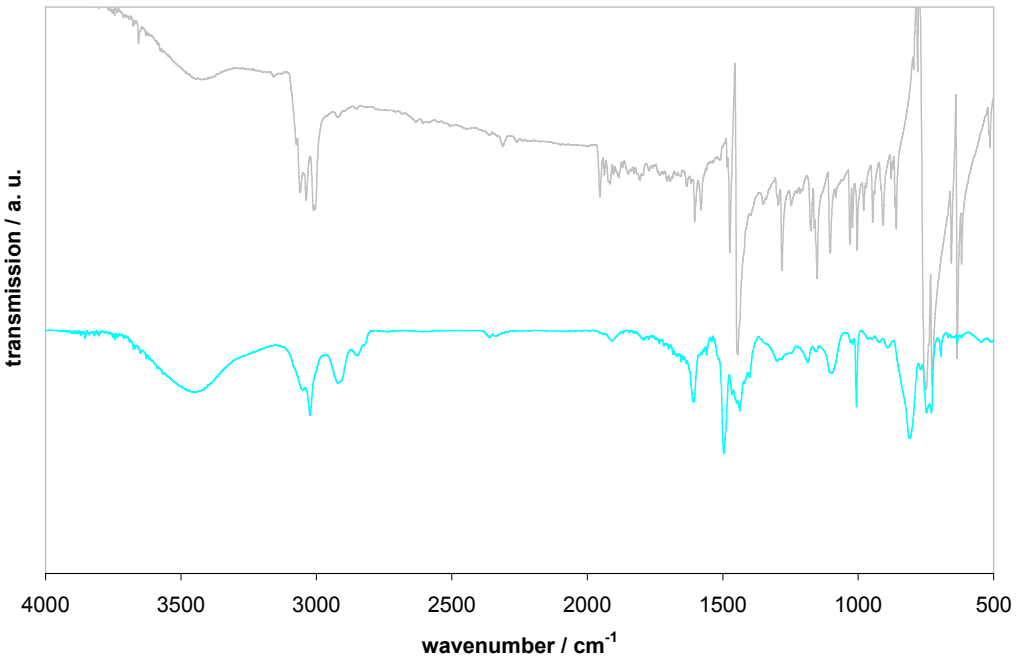

Figure S4. Fourier transform infrared (FTIR) spectra of **sFLUO** and **sFLUO-25**.

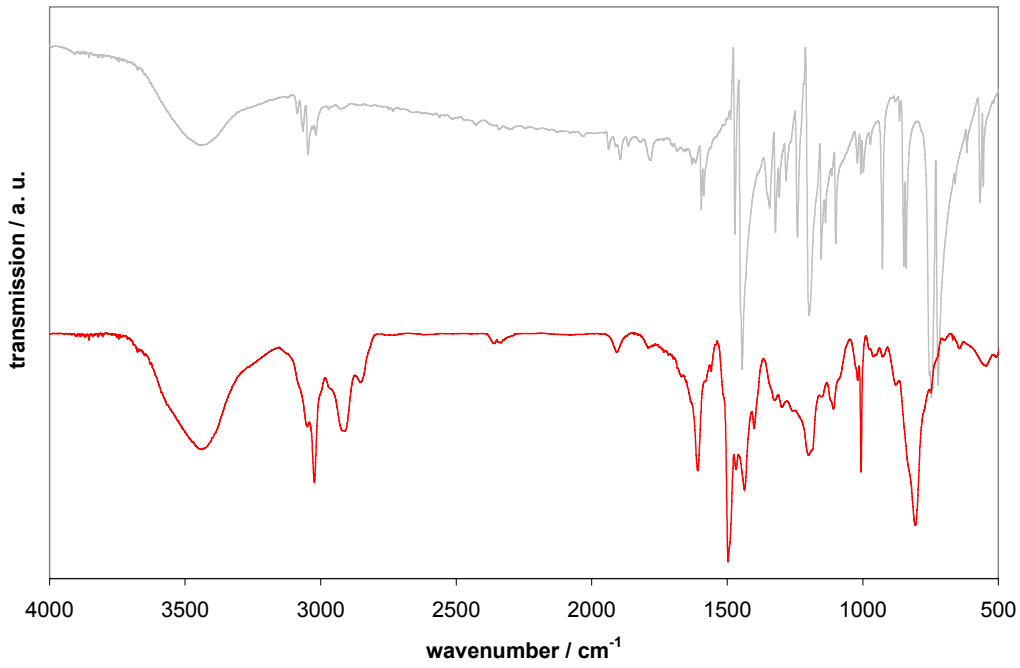

Figure S5. Fourier transform infrared (FTIR) spectra of **DBF** and **DBF-25**.

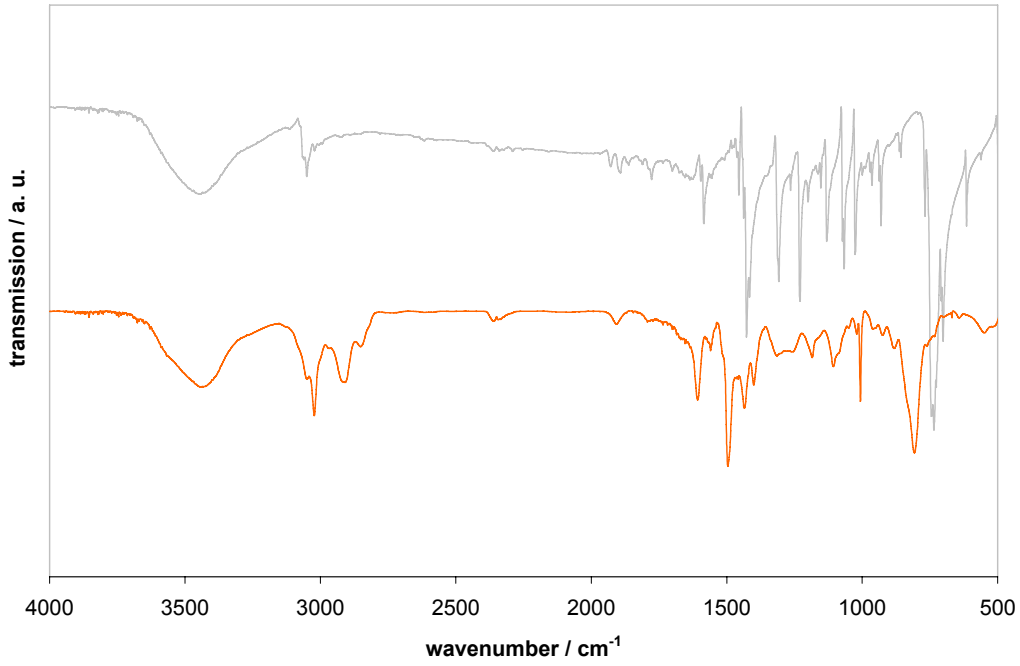

Figure S6. Fourier transform infrared (FTIR) spectra of **DBT** and **DBT-25**.

^{13}C cross-polarization magic angle spinning (CP-MAS) NMR

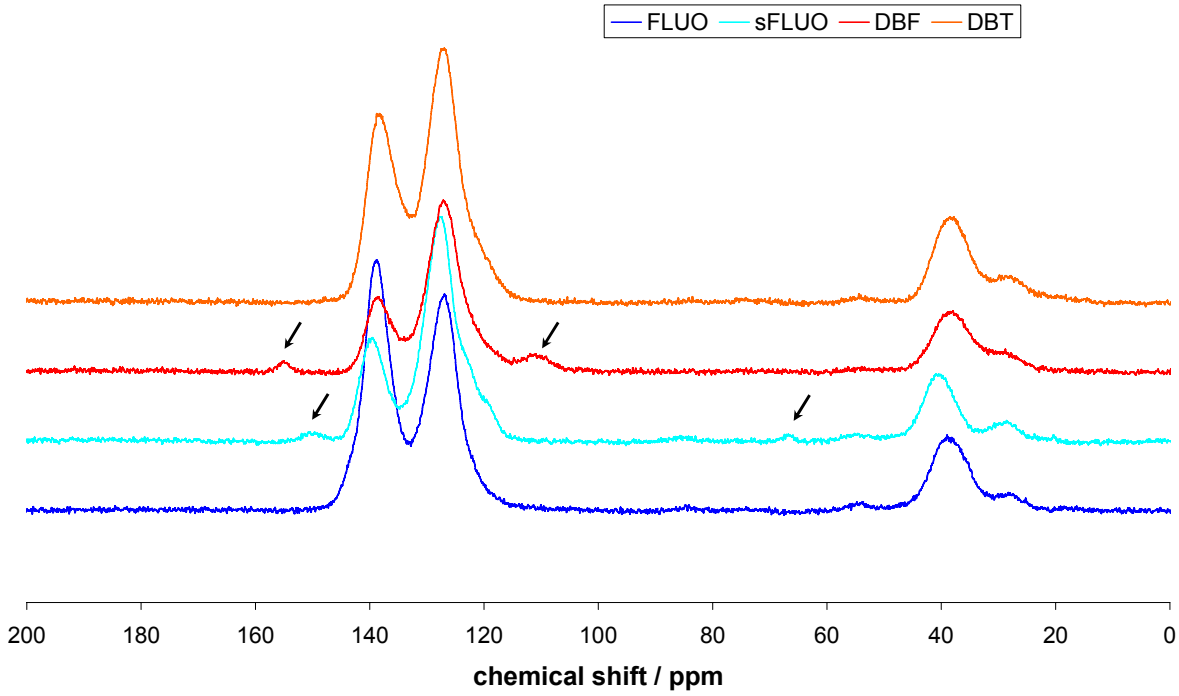

Figure S7. ^{13}C CP-MAS NMR spectra of **FLUO-25**, **sFLUO-25**, **DBF-25** and **DBT-25**.

Nitrogen adsorption analysis

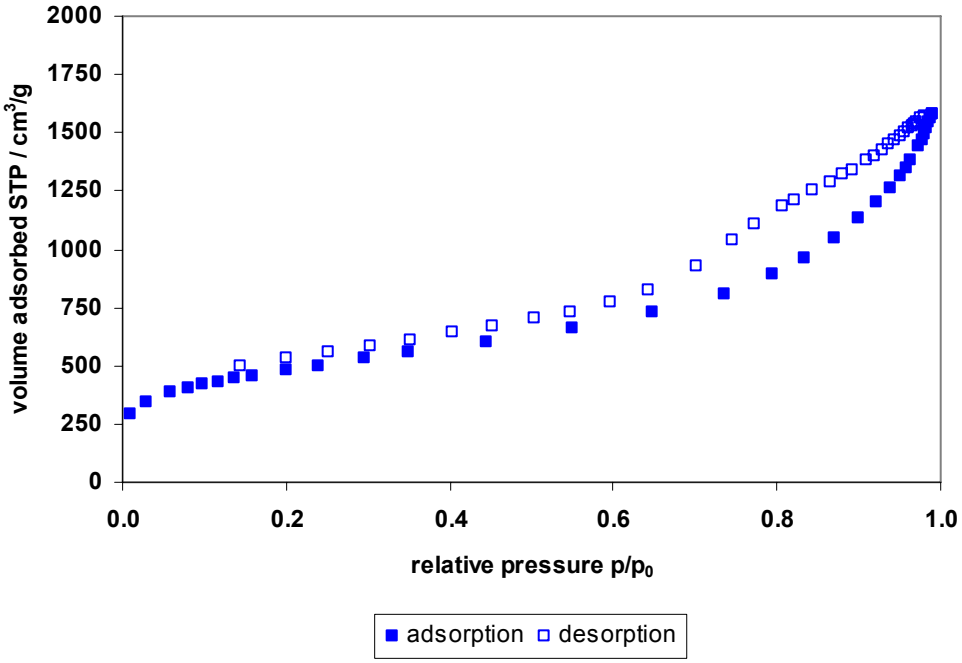

Figure S8. Nitrogen sorption (filled symbols) and desorption (empty symbols) isotherms of **FLUO-10**.

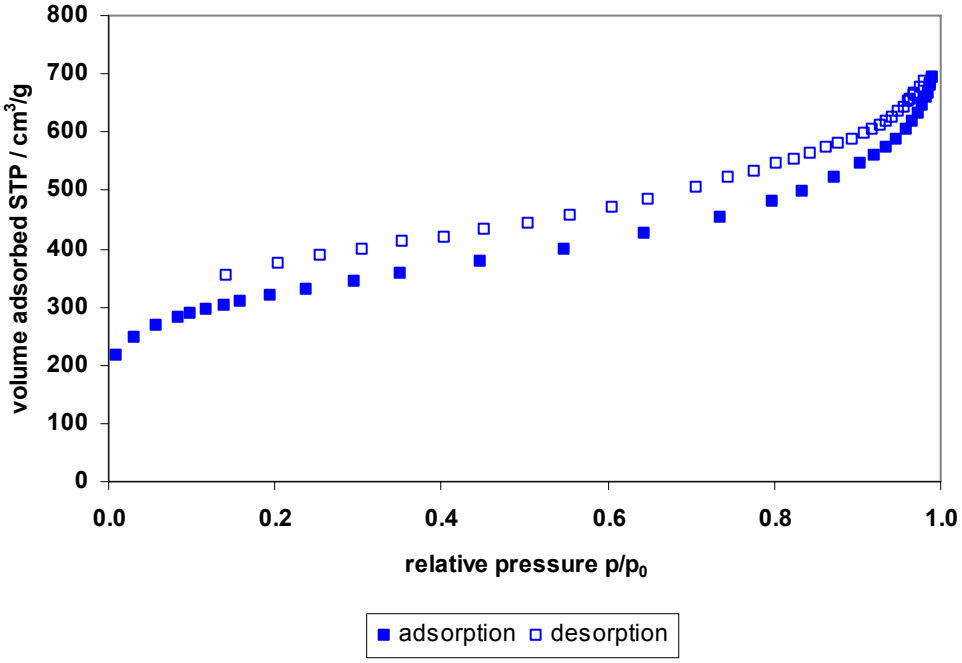

Figure S9. Nitrogen sorption (filled symbols) and desorption (empty symbols) isotherms of **FLUO-25**.

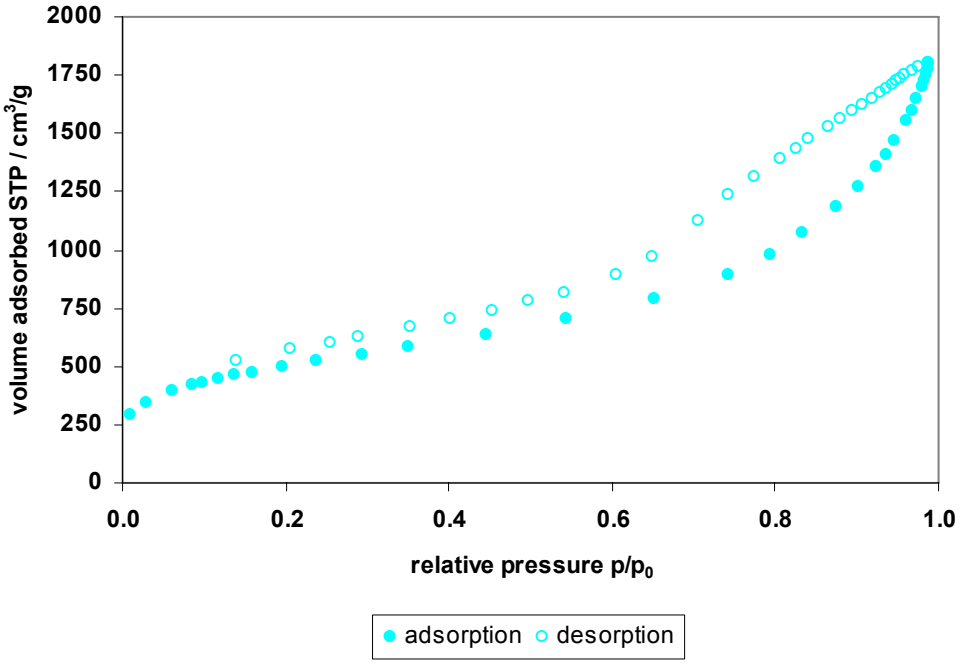

Figure S10. Nitrogen sorption (filled symbols) and desorption (empty symbols) isotherms of **sFLUO-10**.

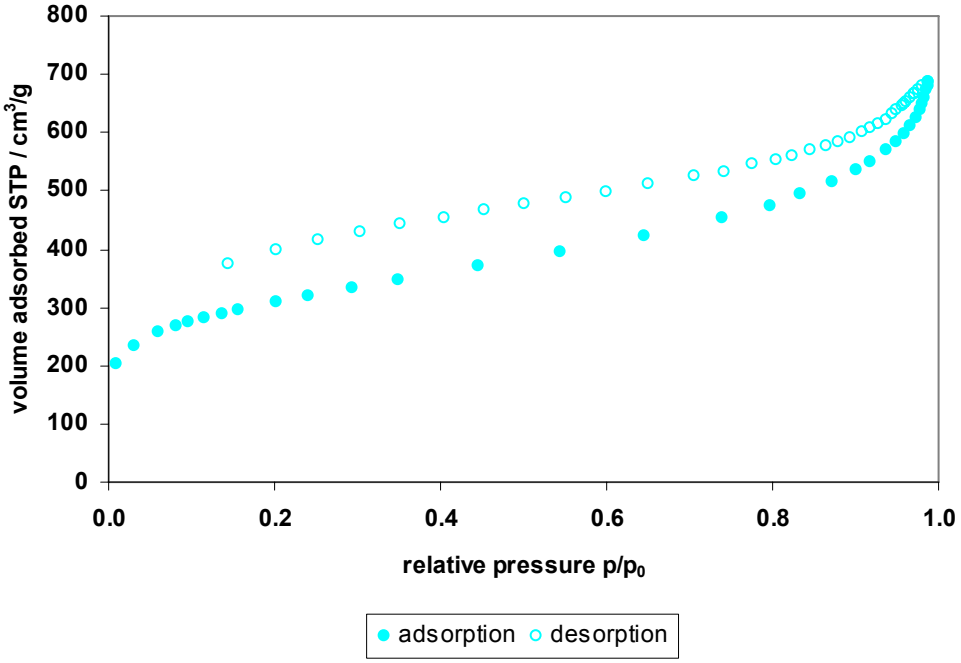

Figure S11. Nitrogen sorption (filled symbols) and desorption (empty symbols) isotherms of **sFLUO-25**.

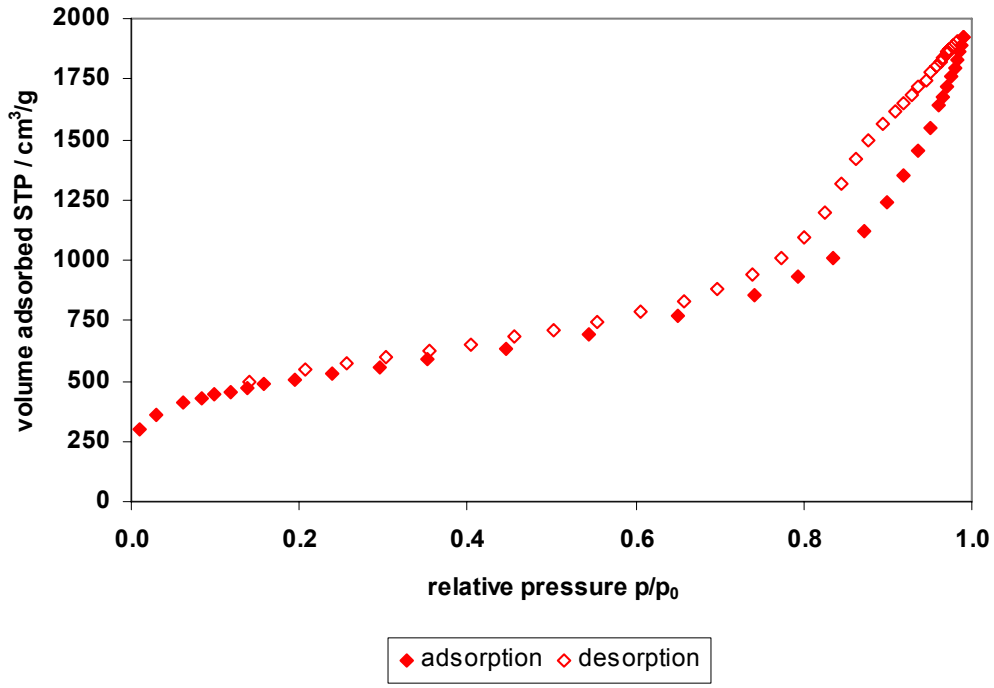

Figure S12. Nitrogen sorption (filled symbols) and desorption (empty symbols) isotherms of **DBF-10**.

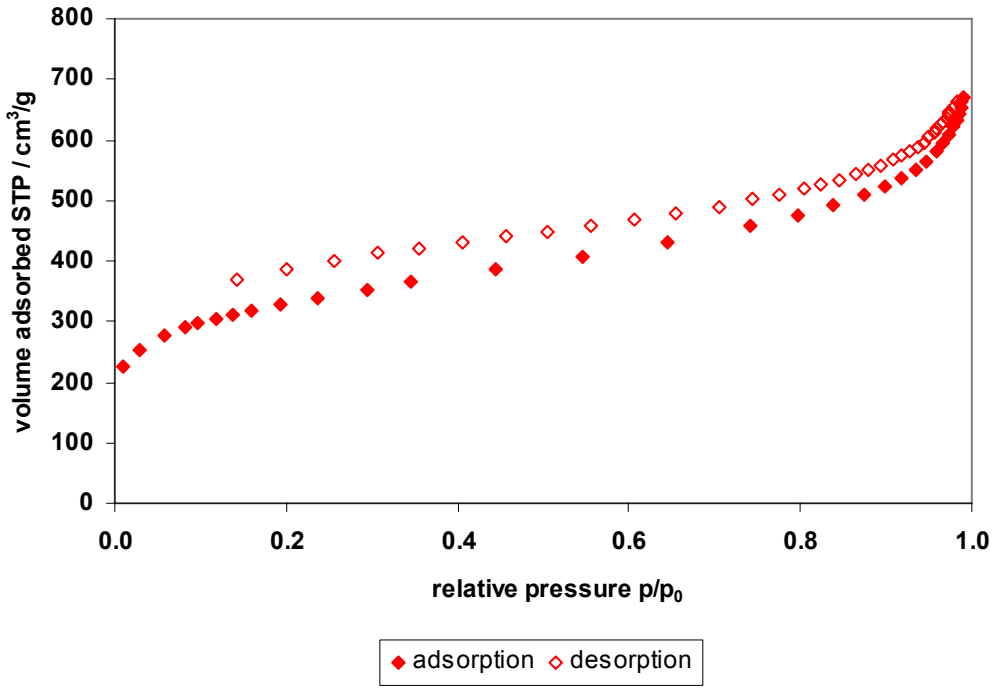

Figure S13. Nitrogen sorption (filled symbols) and desorption (empty symbols) isotherms of **DBF-25**.

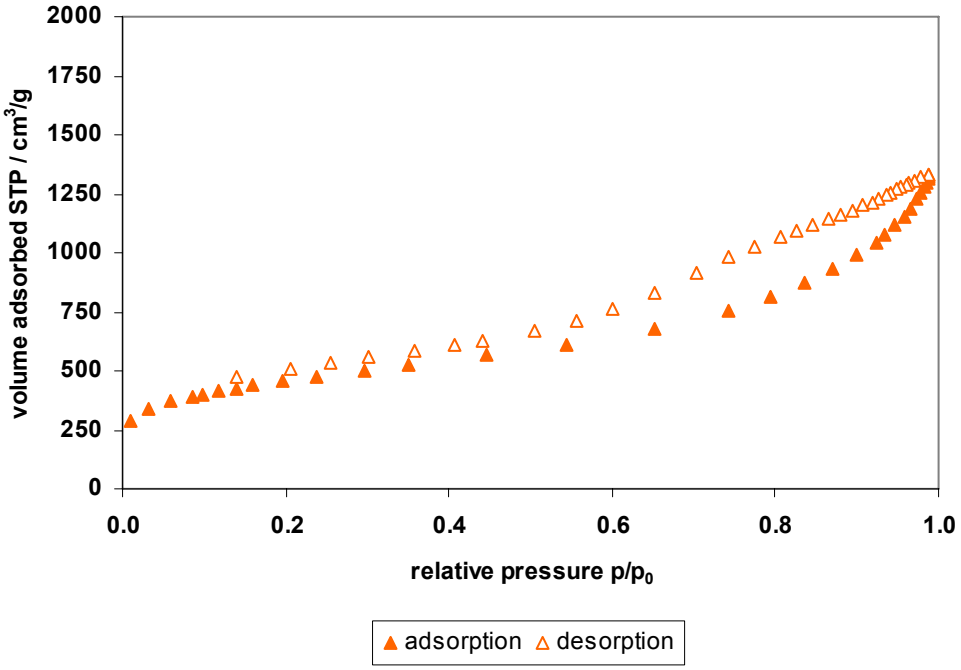

Figure S14. Nitrogen sorption (filled symbols) and desorption (empty symbols) isotherms of **DBT-10**.

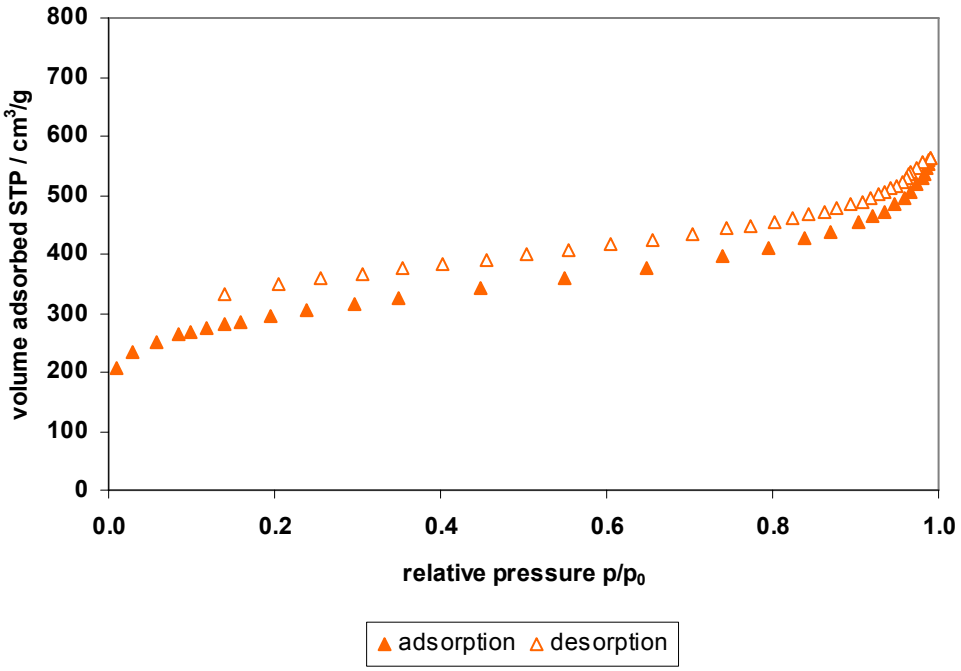

Figure S15. Nitrogen sorption (filled symbols) and desorption (empty symbols) isotherms of **DBT-25**.

Hydrogen adsorption analysis

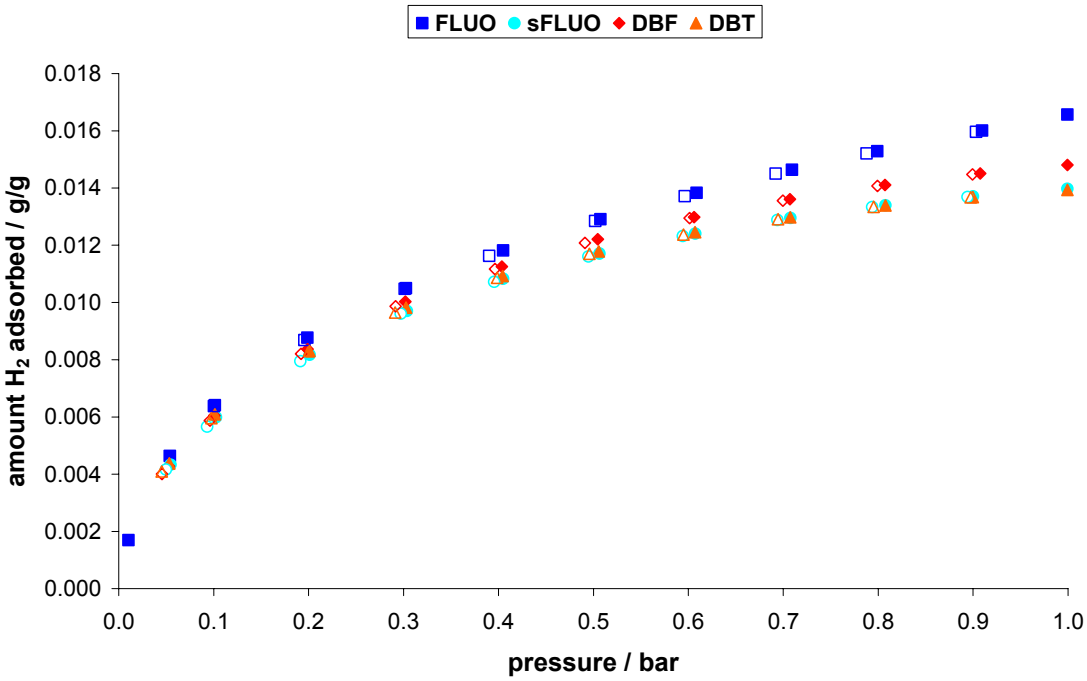

Figure S16. Volumetric hydrogen adsorption (filled) and desorption (empty symbols) isotherms of copolymer networks containing 10 mol% comonomer.

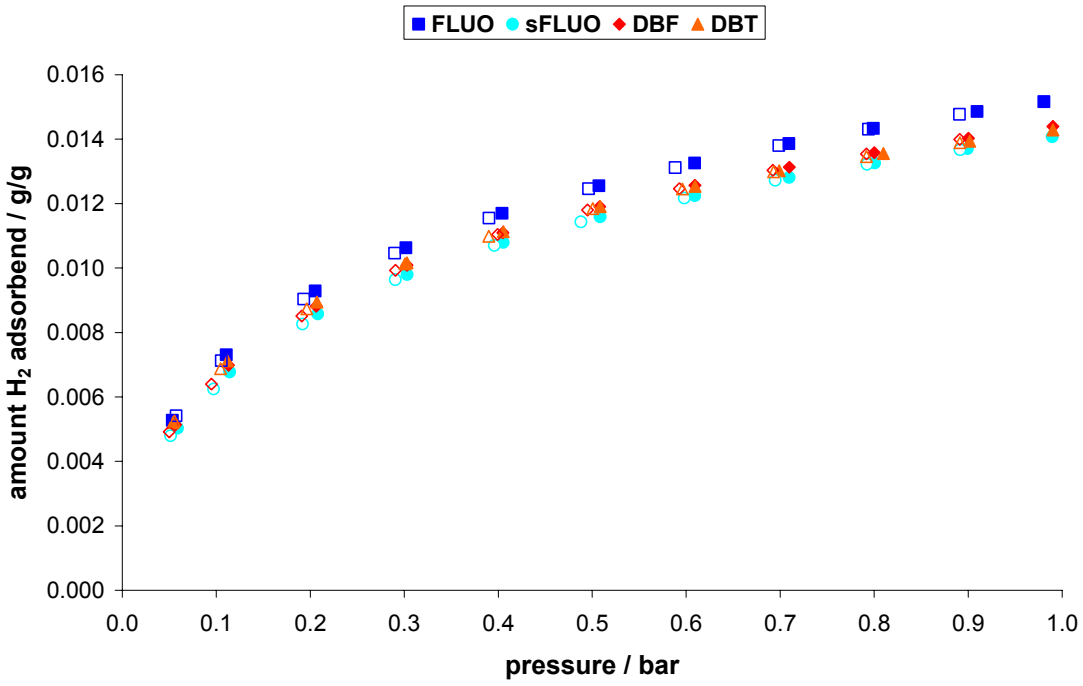

Figure S17. Volumetric hydrogen adsorption (filled) and desorption (empty symbols) isotherms of copolymer networks containing 25 % comonomer.

High pressure methane adsorption analysis

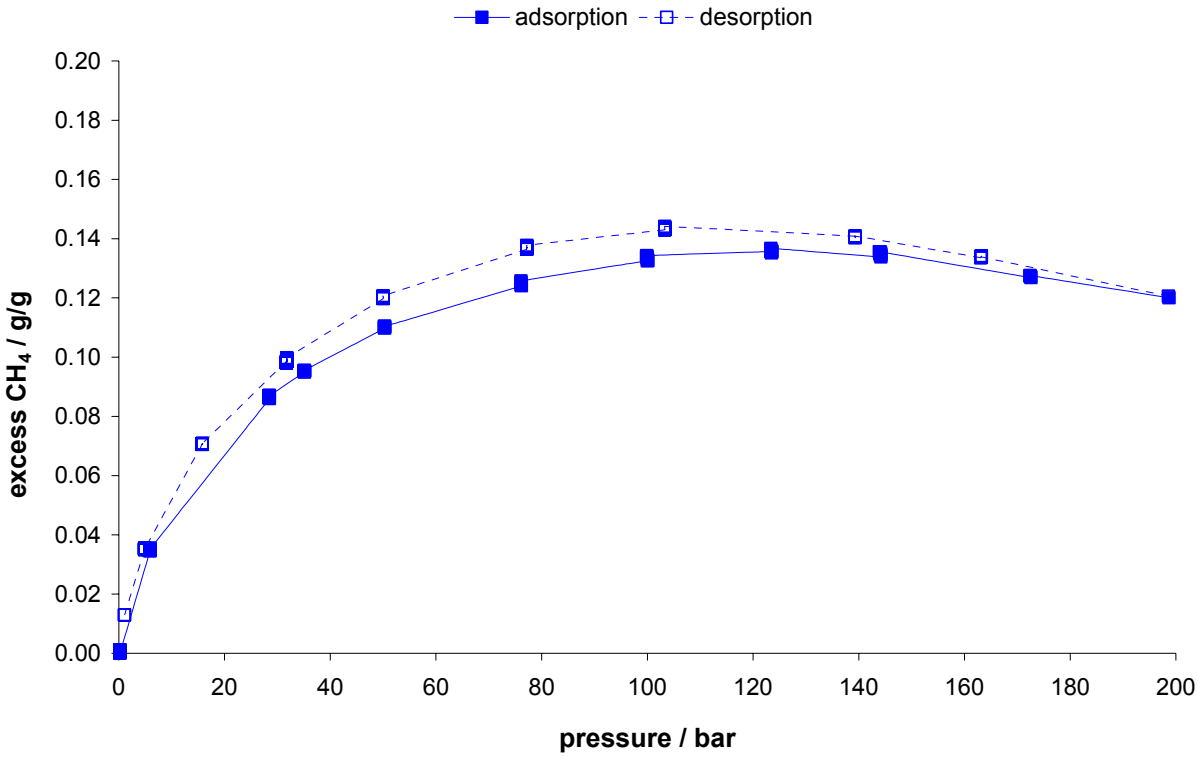

Figure S18. High pressure gravimetric methane adsorption and desorption isotherm of **FLUO-10**.

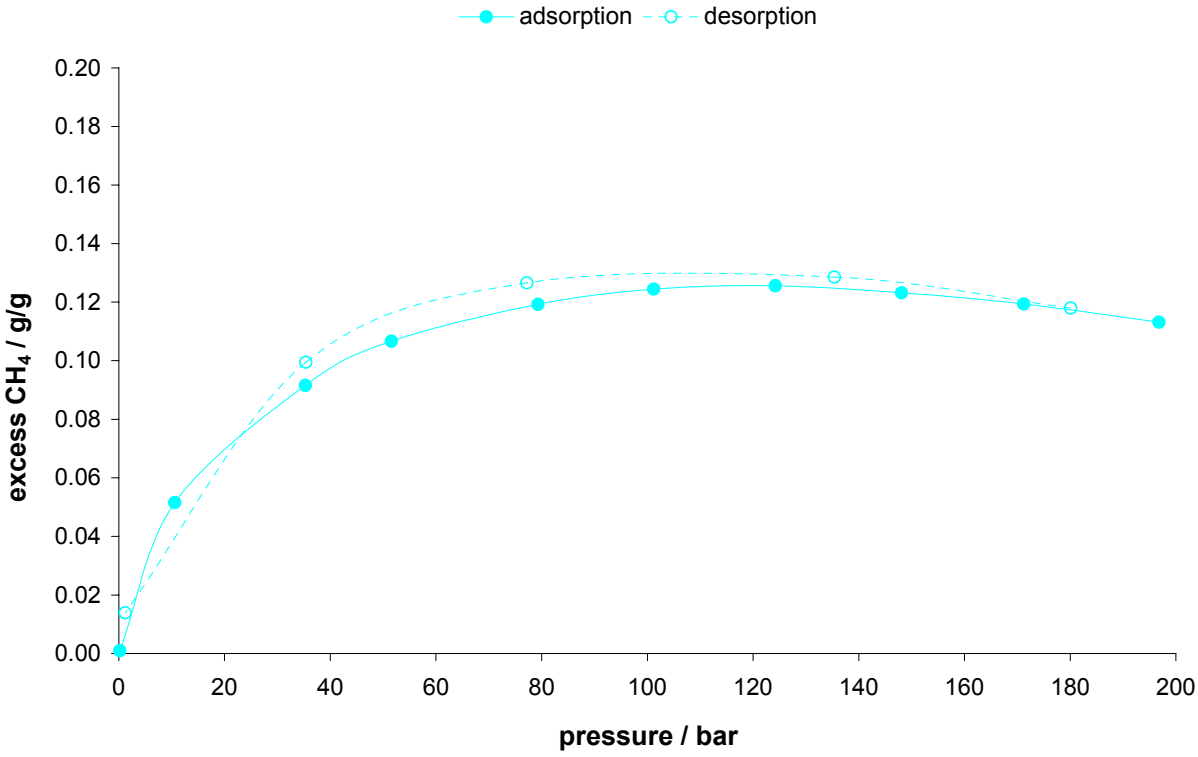

Figure S19. High pressure gravimetric methane adsorption and desorption isotherm of **sFLUO-10**.

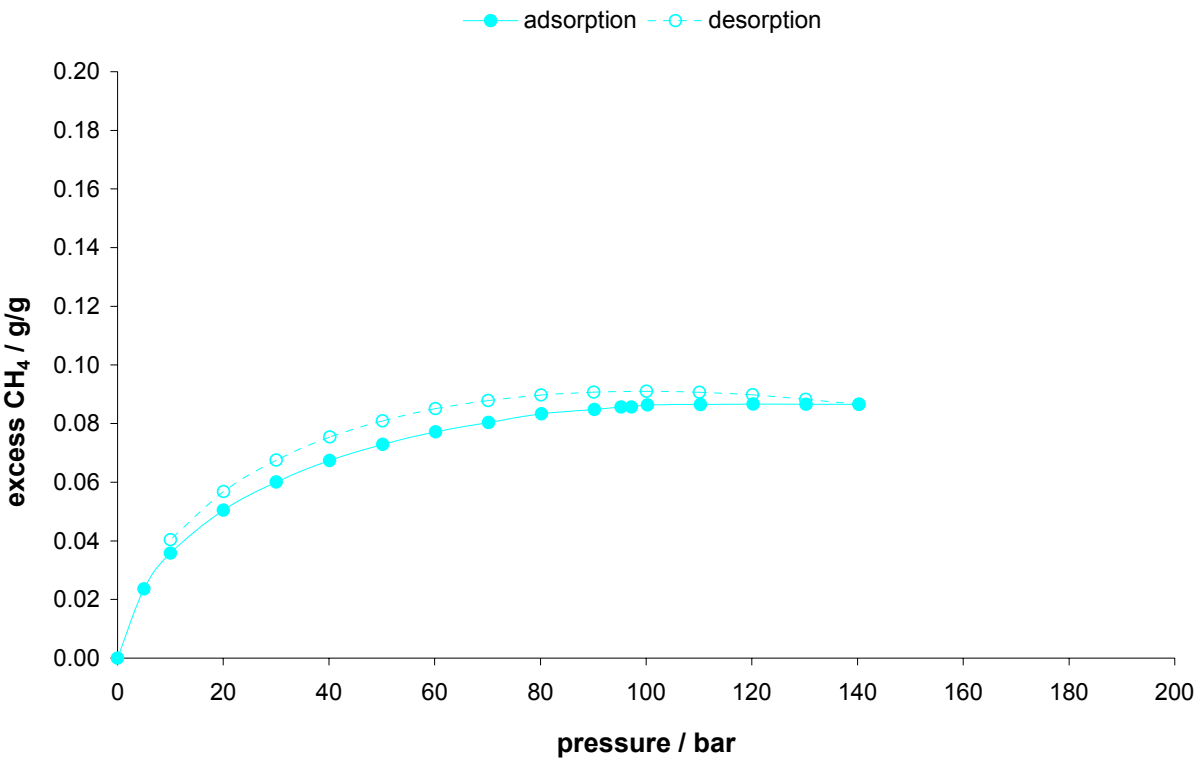

Figure S20. High pressure gravimetric methane adsorption and desorption isotherm of **sFLUO-25**.

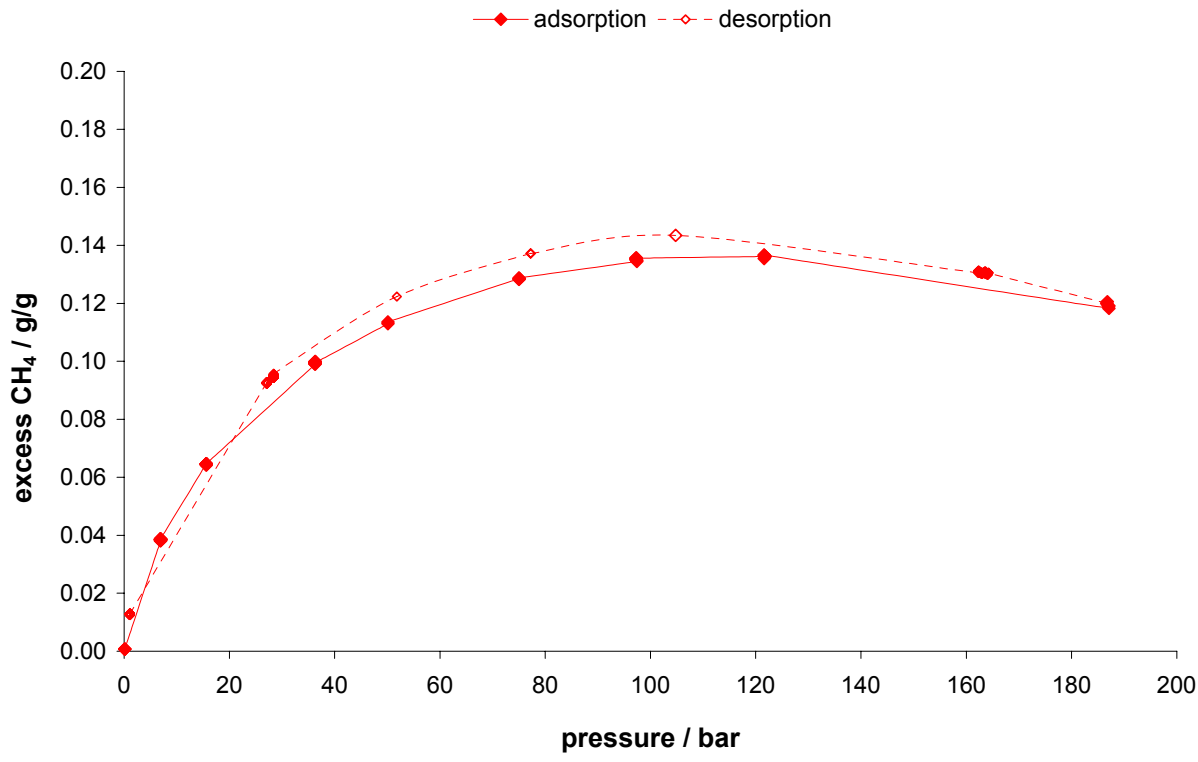

Figure S21. High pressure gravimetric methane adsorption and desorption isotherm of **DBF-10**.

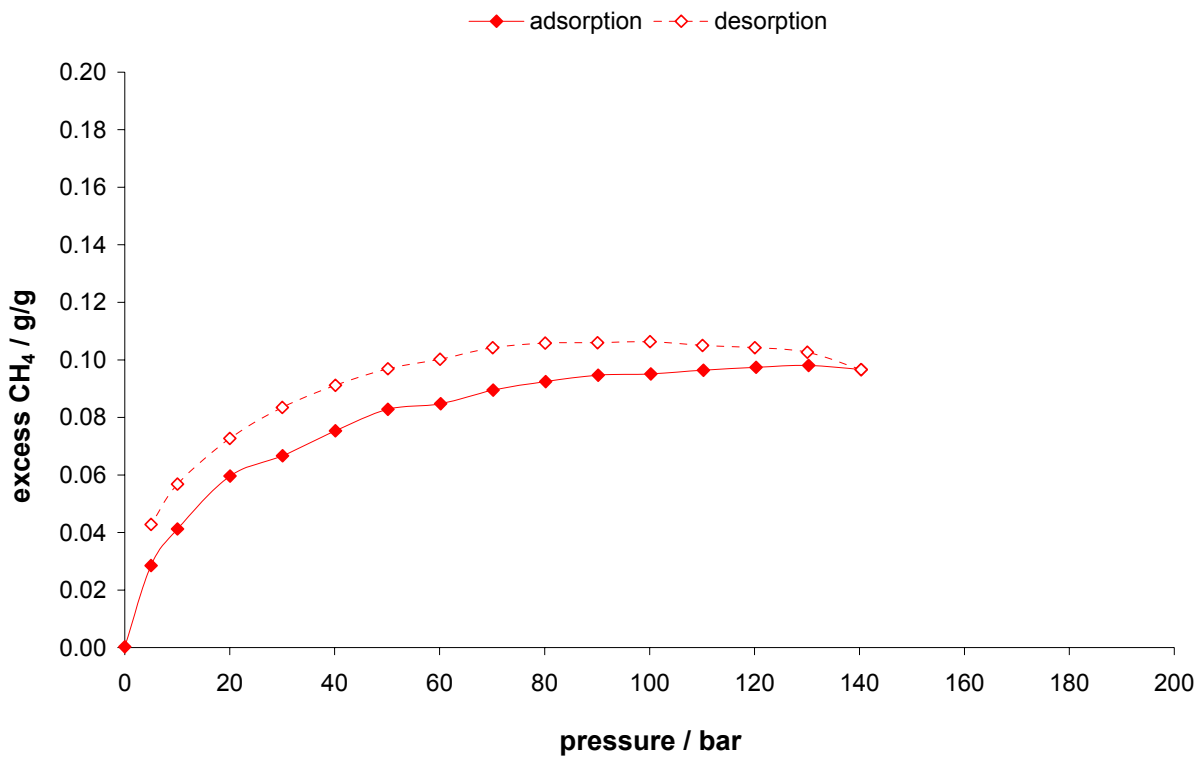

Figure S22. High pressure gravimetric methane adsorption and desorption isotherm of **DBF-25**.

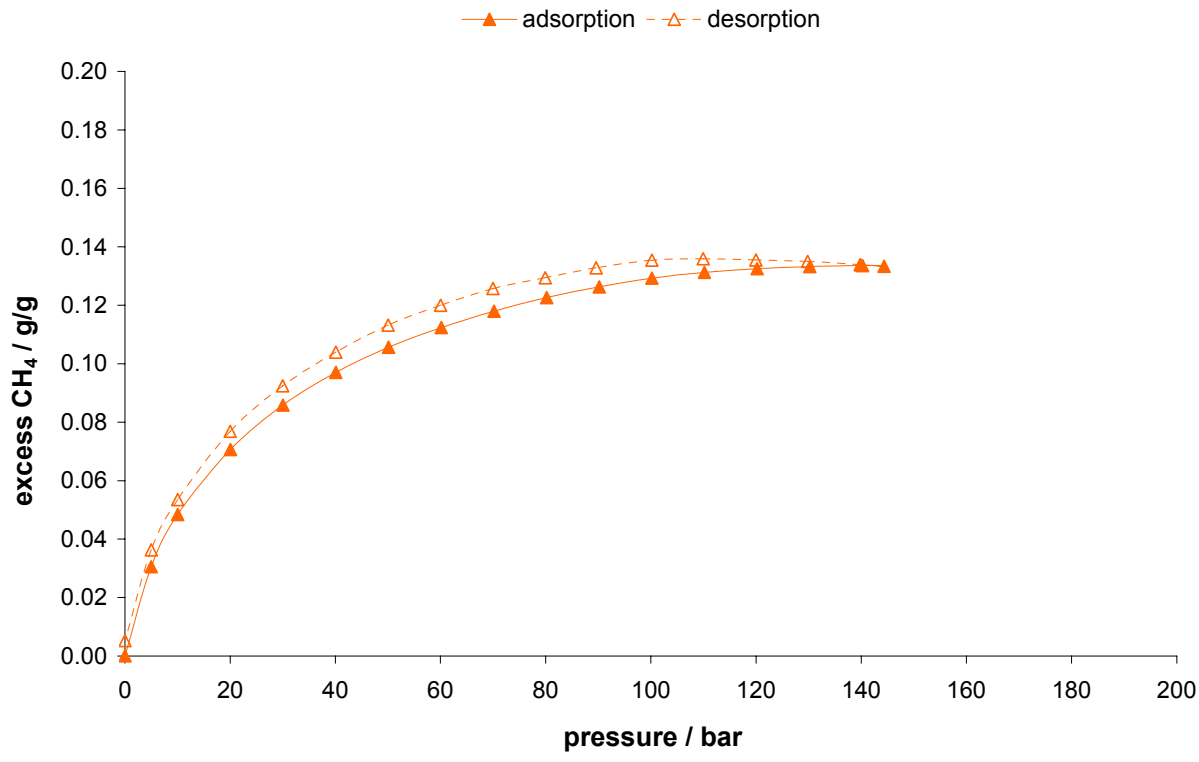

Figure S23. High pressure gravimetric methane adsorption and desorption isotherm of **DBT-10**.

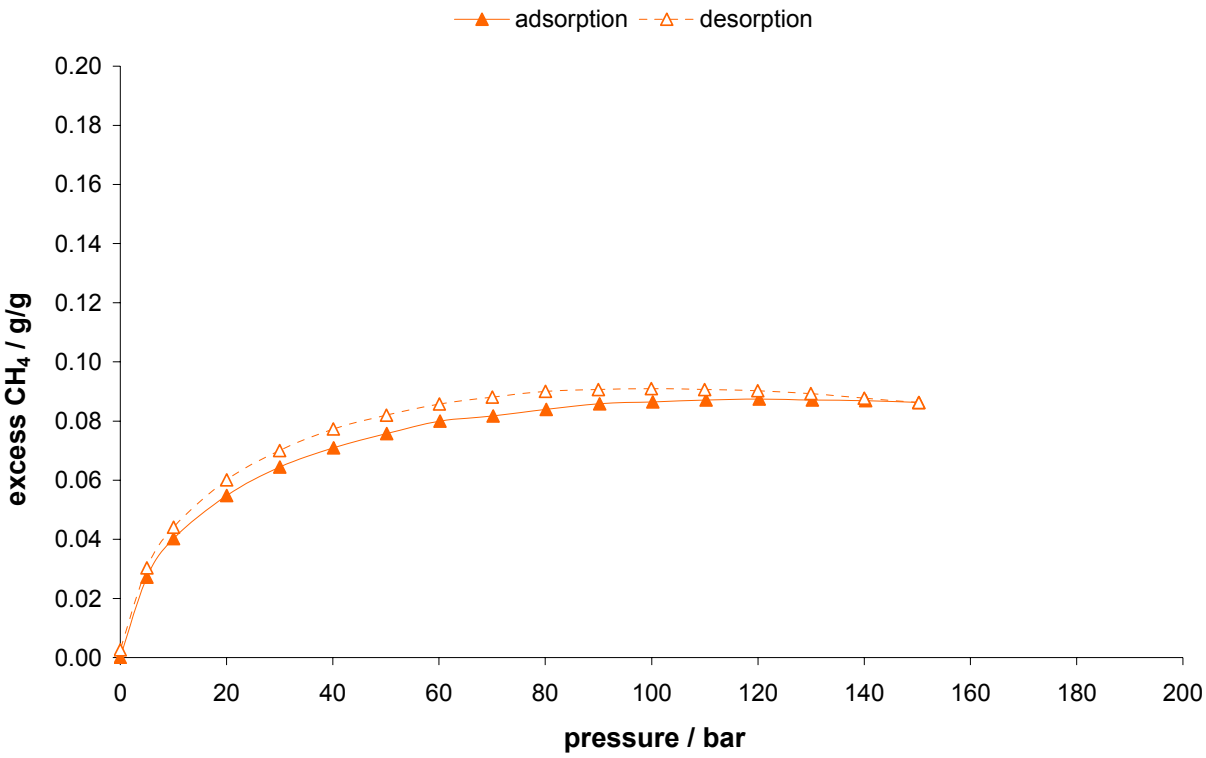

Figure S24. High pressure gravimetric methane adsorption and desorption isotherm of **DBT-25**.

Light-Optical Microscopy (LOM)

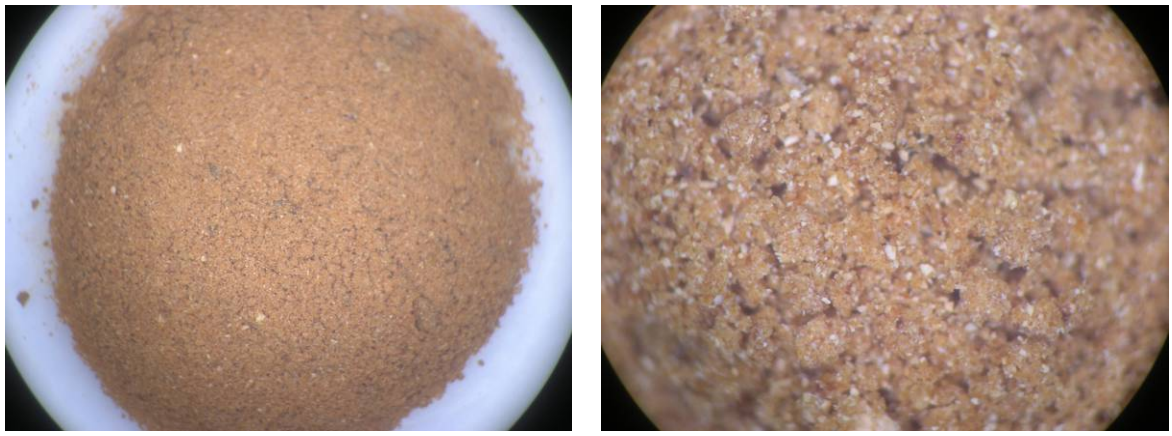

Figure S25. Light-optical micrographs of **FLUO-10**.

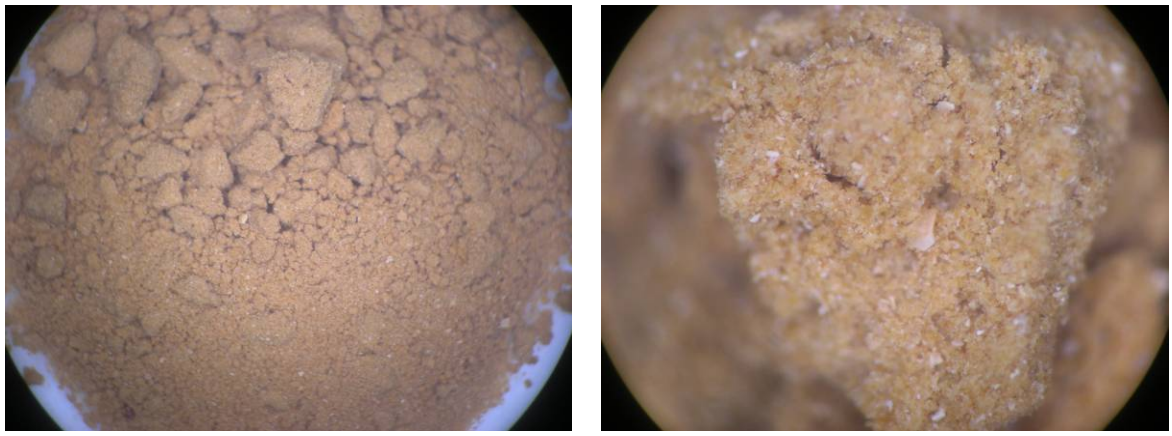

Figure S26. Light-optical micrographs of **sFLUO-10**.

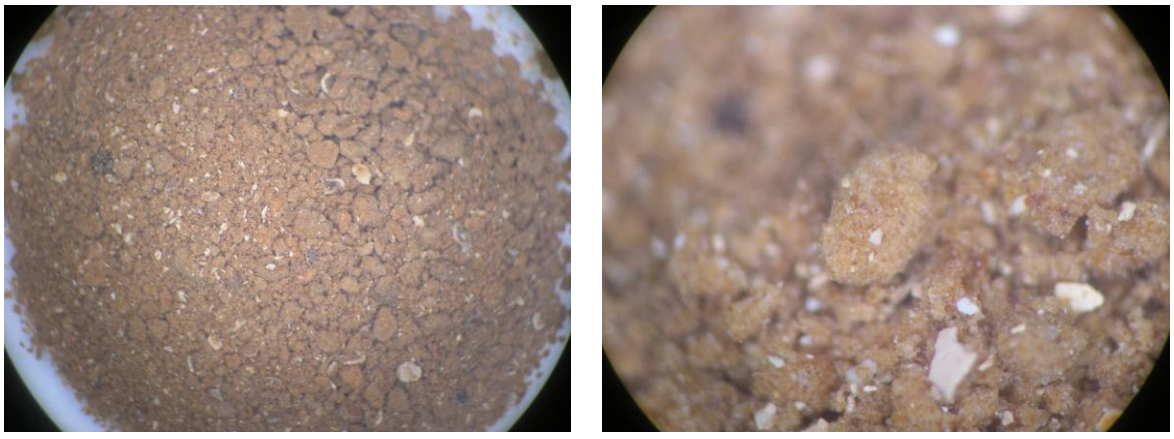

Figure S27. Light-optical micrographs of **DBF-10**.

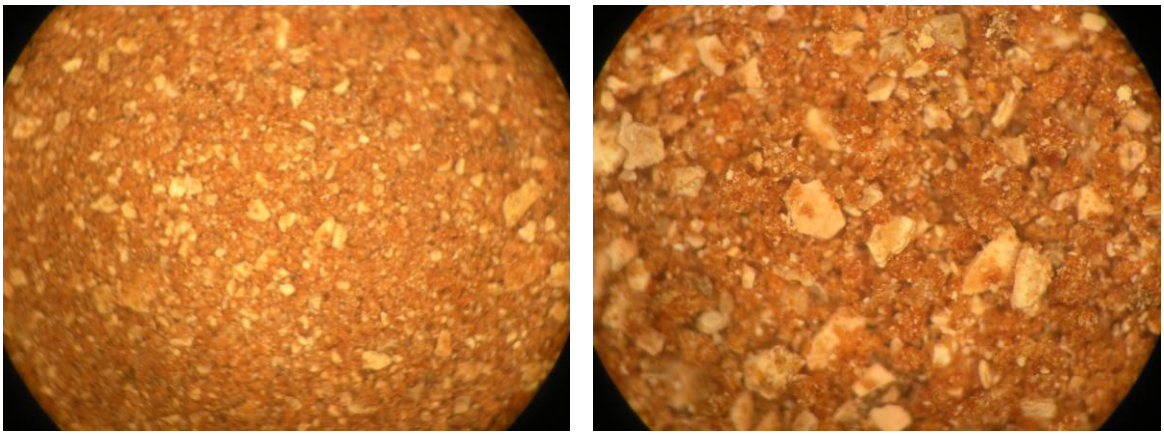

Figure S28. Light-optical micrographs of **DBT-10**.

Scanning Electron Microscopy (SEM)

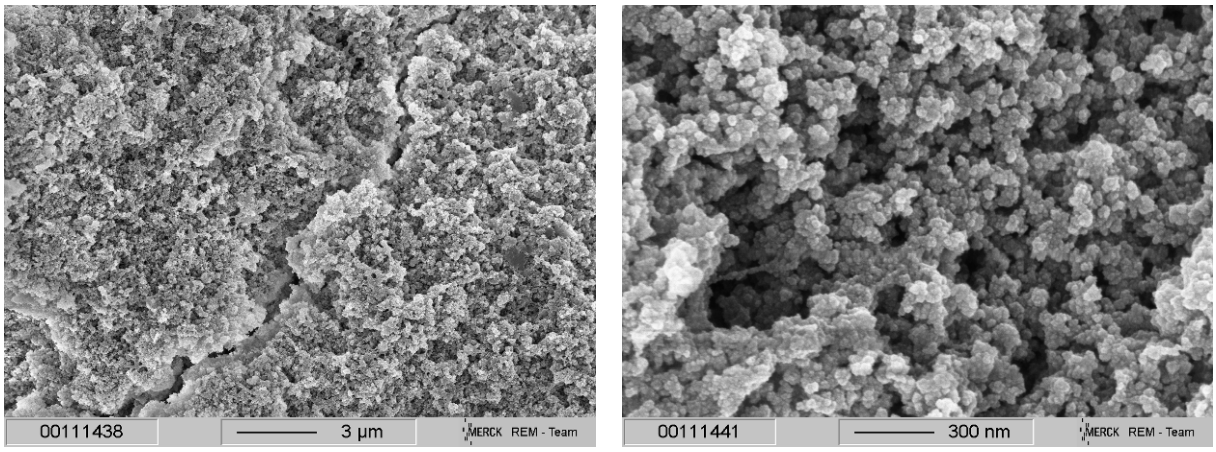

Figure S29. Scanning electron micrographs of **sFLUO-10**.

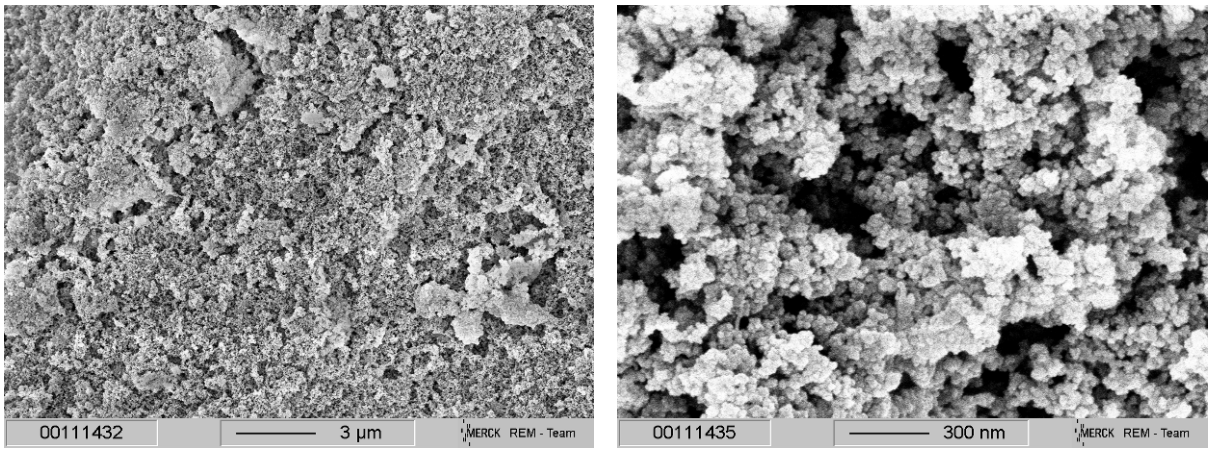

Figure S30. Scanning electron micrographs of **DBF-10**.